PERGAMON

International Journal of Solids and Structures 36 (1999) 1149–1168

INTERNATIONAL JOURNAL OF SOLIDS and STRUCTURES

A differential quadrature procedure for three-dimensional buckling analysis of rectangular plates

T. M. Teo, K. M. Liew*

Division of Engineering Mechanics, School of Mechanical and Production Engineering, Nanyang Technological University, Nanyang Avenue, Singapore 639798

Received 6 May 1997; in revised form 7 November 1997

Abstract

This paper presents an application of the differential quadrature (DQ) method for three-dimensional buckling analysis of rectangular plates. The governing equations of the plate model are first presented in terms of displacement, stress displacement relationship, and boundary conditions with three-dimensional flexibility. These equations are then normalised and discretised using the DQ procedure. Example problems pertaining to the buckling of rectangular plates with generic boundary conditions are selected to illustrate the efficiency and simplicity of implementing the DQ procedure. The convergence characteristics of the method are first conducted based on numerical studies. The DQ solutions are then compared, where possible, with exact or approximate solutions. It is found that the differential quadrature method yields accurate results for the plate problems under the current investigation. In addition to the above, some parametric studies are carried out by varying the plates' aspect ratio, boundary conditions and thickness to width ratio under axial and biaxial loading.

1. Introduction

Exact or analytical solutions for partial differential equations are difficult for many boundary value problems. Hence, numerical methods are widely used in many disciplines of sciences. Some examples of such disciplines are physics, biology and engineering. The most commonly used numerical methods for solving such boundary value problems are the finite element method, finite difference method and boundary element method. These methods usually need a large number of grid points for accurate computation of results even though only a few specified points in the physical domain are required.

Recently, an alternative numerical method, the differential quadrature (DQ) method, was introduced to solve problems in structural mechanics field. It was reported that the DQ method

* Corresponding author.

0020–7683/99/$ - see front matter
PII: S0020–7683(97)00344–2

was able to rapidly compute accurate solutions of partial differential equations by using only a few grid points in the respective solution domains (Bert et al., 1988). The original DQ method was first used in structural mechanics problems by Bert et al. (1988). Later the method was further exploited by Bert et al. (1989) for solving non-linear equations for deflection of orthotropic plates. Despite the increasing application of the DQ method in structural analysis, a drawback regarding its ill-conditioning of the weighting coefficients with increasing number of grid points used, as well as the increasing order of derivatives was pointed out by Bellman (1973), and Civan and Sliepcevich (1983). One way of overcoming this drawback was addressed by Quan and Chang (1989a, b) and followed by Shu and Richards (1992). They introduced a recurrence relationship which is used to generate weighting coefficients for any order of derivatives. Du et al. (1996) employed this method to study the buckling of columns and plates. They solved a fourth order partial differential equation which describes the buckling of columns. The buckling of thin plates using the Classical plate theory was also examined using the DQ method. It was concluded that the DQ method is accurate, efficient and convenient to use and has great potential for wide use in structural analysis. The DQ method by Quan and Chang (1989a, b), and Shu and Richards (1992) for computing the weighting coefficient will be used in this paper.

Numerous methods have been proposed by earlier researchers for solving plate problems on three-dimensional elasticity theory (Srinivas and Rao, 1969, 1970; Iyengar et al., 1974; Hutchinson and Zillimer, 1983; Leissa and Zhang, 1983; Liew et al., 1993, 1994, 1995; Young and Dickinson, 1995). These three-dimensional solutions are extremely useful in evaluating the accuracy of approximate results, for example, in the case of two-dimensional plate theories. In this paper, we employ the DQ method for the eigenvalue solution of three-dimensional buckling analysis of rectangular plates with generic boundary conditions. This article presents the first attempt to apply the DQ method to solve a three-dimensional buckling analysis of rectangular plates.

Numerous researchers have attempted to solve problems related to buckling of plates. Buckling analysis of bi-directional composites and sandwich panels has been reported by Pagano (1970). Brunelle (1971) investigated the buckling behaviour of uniaxially loaded plates under different boundary condition. Bert and Chang (1972) considered the buckling of simply supported rectangular plates. Benson and Hinton (1976) and Hinton (1978) used the finite strip method to solve axially loaded rectangular plates. Roufaeil and Dawe (1982) used the Rayleigh–Ritz method to solve the buckling of Reissner/Mindlin plates. Rao et al. (1975) used a high precision triangle finite element for the problem whereas Cheung et al. (1986) used the finite element method to obtain the buckling load of simply supported plates under axial and shear loading. Doong (1987) used the average stress method to derive a higher-order plate theory for buckling problems. The *p*-Ritz method for buckling analysis of Reissner/Mindlin plates was introduced (Wang et al., 1993; Xiang, 1993).

Srinivas and Rao (1969, 1970) presented the exact three-dimensional buckling solutions of simply supported thick plates. These solutions are invaluable for researchers as they can be used for comparison with other approximate shear deformation theories. They are also invaluable for verifying results produced by other new numerical methods as is the case of this study. Another significant work is due to Wittrick (1987) who obtained the exact three-dimensional solution for eigenvalue problem of buckling of rectangular plates under biaxial compression. In this paper, Wittrick (1987) compared the three-dimensional exact solutions with those from the Mindlin plate theory.

This paper is organised into several sections. In Section 2, the DQ procedures are briefly described. In Section 3, the three-dimensional equilibrium equations, boundary conditions are outlined. In Section 4, the normalisation and discretisation of the three-dimensional linear elasticity equations and boundary conditions are presented. In Section 5, the convergence characteristics and accuracy of the DQ method are demonstrated through the solving of numerical test examples for which the exact solutions or numerical values available are used for comparison. Finally, the conclusions from this study are drawn in Section 6.

2. Differential quadrature method

2.1. *The DQ method for rectangular plates*

The basic idea of the DQ method is to approximate the partial derivatives of a function with respect to a spatial variable at any discrete point as the weighted linear sum of the function values at all the discrete points chosen in the solution domain of spatial variable (Bellman et al., 1972; Civan and Sliepcevich, 1984; Quan and Chang, 1989a). This can be expressed mathematically as:

$$f^n(x_i) = \sum_{j=1}^{N} c_{ij}^{(n)} f(x_j) \quad \text{for } i = 1, 2, 3, \ldots, N \tag{1}$$

where $i = 1, 2, \ldots, N$ are the grid points in the solution domain having N discrete number of points; $f(x_i)$ are the function value at the i-th point; $c_{ij}^{(n)}$ is the weighting coefficients associated with the n-th order partial derivatives of $f(x)$ with respect to x at the discrete point x_i. Such approximation reduces a partial differential equation into a set of algebraic equation for problems independent of time.

The weighting coefficients $c_{ij}^{(n)}$ for $i \neq j$ can be obtained using the following recurrence formulae (Quan and Chang, 1989a, b; Shu and Richards, 1992):

$$c_{ij}^{(n)} = n\left(c_{ij}^{(n-1)} c_{ij}^{(1)} - \frac{c_{ij}^{(n-1)}}{x_i - x_j}\right) n = 2, 3, \ldots, N-1; \quad i, j = 1, 2, 3, \ldots, N \tag{2a}$$

where $c_{ij}^{(1)}$ is given as:

$$c_{ij}^{(1)} = \frac{M^{(1)}(x_i)}{(x_i - x_j) M^{(1)}(x_j)} \quad i, j = 1, 2, 3, \ldots, N \tag{2b}$$

The weighting coefficients when $i = j$ are given as:

$$c_{ii}^{(n)} = -\sum_{j=1, j\neq i}^{N} c_{ij}^{(n)} \quad \text{for } i = 1, 2, 3, \ldots, N; \quad n = 1, 2, 3, \ldots, N-1 \tag{2c}$$

For eqn (2b), $M^{(1)}$ is denoted by the following expression:

$$M^{(1)}(x_k) = \prod_{j=1, j\neq k}^{N} (x_k - x_j) \quad \text{for } k = 1, 2, 3, \ldots, N \tag{3}$$

The above DQ approximation is shown for a one-dimensional case. The three-dimensional DQ approximation can be easily extended from the one-dimensional case. For the first-order derivatives of the function $f(x, y, z)$ can be approximated as

$$\left.\frac{\partial f}{\partial x}\right|_{ijk} \approx \sum_{l=1}^{Nx} A_{il}^{(1)} f_{ljk}; \quad \left.\frac{\partial f}{\partial y}\right|_{ijk} \approx \sum_{m=1}^{Ny} B_{jm}^{(1)} f_{imk}; \quad \left.\frac{\partial f}{\partial z}\right|_{ijk} \approx \sum_{n=1}^{Nz} C_{kn}^{(1)} f_{ijn} \tag{4a–c}$$

The second-order derivatives of the function $f(x, y, z)$ can be approximated as

$$\left.\frac{\partial^2 f}{\partial x^2}\right|_{ijk} \approx \sum_{l=1}^{Nx} A_{il}^{(2)} f_{ljk}; \quad \left.\frac{\partial^2 f}{\partial y^2}\right|_{ijk} \approx \sum_{m=1}^{Ny} B_{jm}^{(2)} f_{imk}; \quad \left.\frac{\partial^2 f}{\partial z^2}\right|_{ijk} \approx \sum_{n=1}^{Nz} C_{kn}^{(2)} f_{ijn} \tag{5a–c}$$

$$\left.\frac{\partial}{\partial x}\left(\frac{\partial f}{\partial y}\right)\right|_{ijk} \approx \sum_{l=1}^{Nx} A_{il}^{(1)} \sum_{m=1}^{Ny} B_{jm}^{(1)} f_{lmk}; \quad \left.\frac{\partial}{\partial x}\left(\frac{\partial f}{\partial z}\right)\right|_{ijk} \approx \sum_{l=1}^{Nx} A_{il}^{(1)} \sum_{n=1}^{Nz} C_{kn}^{(1)} f_{ljn} \tag{6a–b}$$

$$\left.\frac{\partial}{\partial y}\left(\frac{\partial f}{\partial z}\right)\right|_{ijk} \approx \sum_{m=1}^{Ny} B_{jm}^{(1)} \sum_{n=1}^{Nz} C_{kn}^{(1)} f_{imn} \tag{6c}$$

In the above approximations [eqns (4)–(6)], A, B and C denote the weighting coefficients of the partial derivative of the function $f(x, y, z)$ with respect to the x, y and z directions.

2.2. *Additional comments on the DQ method*

This paper presents the DQ solution only for plates in a rectangular domain. It should be noted that the DQ method can also be used to solve plate problems with more complex geometry. There are basically two methods for doing this. The first method is to use the four node or eight node DQ method (Liew and Han, 1997; Han and Liew, 1997). The basic idea of this method is to map an arbitrary straight or curvilinear sided plate onto a basic square domain using the four or eight node geometric co-ordinate transformation technique. The solution of the problem can then be obtained by solving the geometrically transformed governing equation. The second method of solving plate problems of arbitrary shape is to extend the DQ method into the differential quadrature element method (DQEM) (Liu et al., 1997). The basic idea of the DQEM is first to divide the whole variable domain into several sub-domains, called elements, in which each element is discretised using the DQ procedure. All the discretised elements are then assembled in the overall characteristic equations from which the solution is acquired.

3. Basic governing equations

3.1. *Equilibrium equations*

The equations of equilibrium in terms of displacement for a homogeneous isotropic plate without the body force can be written as (Wittrick, 1987):

$$\nabla^2 u + \frac{1}{1-2v}\frac{\partial e}{\partial x} - \frac{2P_x(1-v)}{E}\left[\frac{\partial^2 u}{\partial x^2} + \phi\frac{\partial^2 u}{\partial y^2}\right] = 0 \tag{7a}$$

$$\nabla^2 v + \frac{1}{1-2v}\frac{\partial e}{\partial y} - \frac{2P_x(1-v)}{E}\left[\frac{\partial^2 v}{\partial x^2} + \phi\frac{\partial^2 v}{\partial y^2}\right] = 0 \tag{7b}$$

$$\nabla^2 w + \frac{1}{1-2v}\frac{\partial e}{\partial z} - \frac{2P_x(1-v)}{E}\left[\frac{\partial^2 w}{\partial x^2} + \phi\frac{\partial^2 w}{\partial y^2}\right] = 0 \tag{7c}$$

where e is the dilatation, defined by

$$e = (\partial/\partial x; \partial/\partial y; \partial/\partial z)\{u, v, w\}^T \tag{8}$$

Also, ϕ is the ratio of the destabilising effect of the x-direction, P_x, to the destabilising effect of the y-direction, P_y. It is defined by the following relationship:

$$\phi P_x = P_y \tag{9}$$

The variables u, v and w are the displacements in the x, y and z-directions as depicted in the co-ordinate system shown in Fig. 1. The symbol v represents the Poisson ratio of the plate and E the Young's modulus of the plate.

The relationship between the stress components and the displacements is given as:

$$\begin{bmatrix} \sigma_x \\ \sigma_y \\ \sigma_z \\ \tau_{xy} \\ \tau_{xz} \\ \tau_{yz} \end{bmatrix} = \begin{bmatrix} \varphi(1-v)\frac{\partial}{\partial x} & \varphi v\frac{\partial}{\partial y} & \varphi v\frac{\partial}{\partial z} \\ \varphi v\frac{\partial}{\partial x} & \varphi(1-v)\frac{\partial}{\partial y} & \varphi v\frac{\partial}{\partial z} \\ \varphi v\frac{\partial}{\partial x} & \varphi v\frac{\partial}{\partial y} & \varphi(1-v)\frac{\partial}{\partial z} \\ G\frac{\partial}{\partial y} & G\frac{\partial}{\partial x} & 0 \\ G\frac{\partial}{\partial z} & 0 & G\frac{\partial}{\partial x} \\ 0 & G\frac{\partial}{\partial z} & G\frac{\partial}{\partial y} \end{bmatrix} \times \begin{bmatrix} u \\ v \\ w \end{bmatrix} \tag{10a}$$

where

$$\varphi = \frac{2G}{(1-2v)}; \quad G = \frac{E}{2(1+v)} \tag{10b–c}$$

In the above equations, σ_x, σ_y and σ_z represents the stress in the x, y and z-directions respectively; τ_{xy}, τ_{xz} and τ_{yx} are the shear stresses in the x–y, x–z and y–z directions; and G is the shear modulus of the plate.

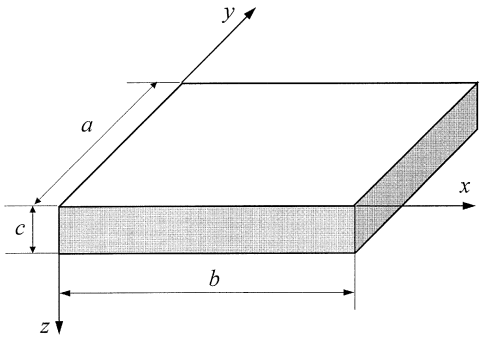

Fig. 1. Coordinate system and dimensions.

3.2. *Boundary conditions*

For three-dimensional analysis of a plate, the boundary conditions need to be applied to all six faces of the solid. The four faces where $x = 0$, a and $y = 0$, b are called the edge boundary conditions whereas the top and bottom surfaces of the plate are called the surface boundary conditions. In this paper, the free surface boundary conditions shall be used for all the examples considered. The three types of edge boundary conditions considered are namely the fully clamped edge boundary condition (C), the simply supported edge boundary conditions (S) and the free edge boundary condition (F).

The equations describing the boundary conditions are as follows:

- Clamped edge boundary condition (C)

$$u = 0; \quad v = 0; \quad w = 0 \tag{11}$$

- Simply supported edge boundary condition (S)

$$\text{On } x = 0 \quad \text{and} \quad a: \quad \sigma_x = 0; \quad v = 0; \quad w = 0 \tag{12a}$$

$$\text{On } y = 0 \quad \text{and} \quad b: \quad \sigma_y = 0; \quad u = 0; \quad w = 0 \tag{12b}$$

- Free edge boundary condition (F)

$$\text{On } x = 0 \quad \text{and} \quad a: \quad \sigma_x = 0; \quad \tau_{xy} = 0; \quad \tau_{xz} = 0 \tag{13a}$$

$$\text{On } y = 0 \quad \text{and} \quad b: \quad \sigma_y = 0; \quad \tau_{xy} = 0; \quad \tau_{yz} = 0 \tag{13b}$$

- Free surface boundary condition

$$\text{On } z = 0 \quad \text{and} \quad c: \quad \sigma_z = 0; \quad \tau_{xz} = 0; \quad \tau_{yz} = 0 \tag{14}$$

4. Numerical implementation

The loading conditions of the plate are shown in Fig. 2. Figure 2a shows the uniaxial loading of a plate whereas Fig. 2b shows the biaxial loading of the plate. For the purpose of describing the

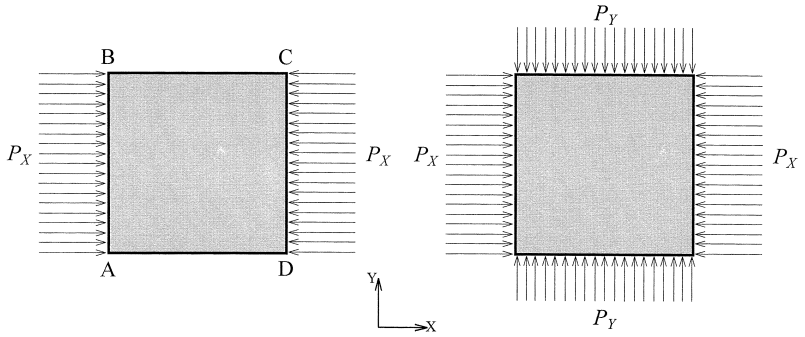

Fig. 2. Geometry and loading condition of plate.

boundary conditions, the notation SCSF is used to denote a plate with edges AB and CD simply supported (S), BC clamped (C) and DA free (F).

In order to normalise the above equations, the following non-dimensional parameters are introduced

$$X = \frac{x}{a}; \quad Y = \frac{y}{b}; \quad Z = \frac{z}{c}; \tag{15a–c}$$

$$U = \frac{u}{a}; \quad V = \frac{v}{b}; \quad W = \frac{w}{a}; \tag{15d–f}$$

$$\alpha = \frac{a}{b}; \quad \beta = \frac{c}{b}; \quad \gamma = \frac{c}{a}; \tag{15g–i}$$

$$\tau_{XY} = \frac{\tau_{xy}}{G}; \quad \tau_{XZ} = \frac{\tau_{xz}}{G}; \quad \tau_{YZ} = \frac{\tau_{yz}}{G}; \tag{15j–l}$$

$$\sigma_X = \frac{\gamma(1-2v)\sigma_x}{2G}; \quad \sigma_Y = \frac{\gamma(1-2v)\sigma_y}{2G}; \quad \sigma_Z = \frac{\gamma(1-2v)\sigma_z}{2G} \tag{15m–o}$$

In the above equations, a, b and c represent the length in the x, y and z-directions of the plate, respectively.

4.1. *Normalisation and discretisation of the equilibrium equations*

By substituting eqns (15) into the equilibrium equations [eqns (7)] applying the DQ procedure described in Section 2.1, the governing equations can be discretised as:

$$2\gamma^2(1-v)\sum_{l=1}^{N_X} A_{il}^{(2)} U_{ljk} - \beta^2(1-2v)\sum_{m=1}^{N_Y} B_{jm}^{(2)} U_{imk} + (1-2v)\sum_{n=1}^{N_Z} C_{kn}^{(2)} U_{ijn}$$

$$+\gamma^2 \sum_{l=1}^{N_X} A_{il}^{(1)} \sum_{m=1}^{N_Y} B_{jm}^{(1)} V_{lmk} + \gamma \sum_{l=1}^{N_X} A_{il}^{(1)} \sum_{n=1}^{N_Z} C_{kn}^{(1)} W_{ljn}$$

$$= \frac{2P_x(1-v)(1-2v)}{E} \left[\gamma^2 \sum_{l=1}^{N_X} A_{il}^{(2)} U_{ljk} + \phi\beta^2 \sum_{m=1}^{N_Y} B_{jm}^{(2)} U_{imk} \right] \quad (16)$$

$$\beta^2 \sum_{l=1}^{N_X} A_{il}^{(1)} \sum_{m=1}^{N_Y} B_{jm}^{(1)} U_{lmk} + \gamma^2(1-2v) \sum_{l=1}^{N_X} A_{il}^{(2)} V_{ljk} + 2\beta^2(1-v) \sum_{m=1}^{N_Y} B_{jm}^{(2)} V_{imk}$$

$$+(1-2v) \sum_{n=1}^{N_Z} C_{kn}^{(2)} V_{ijn} + \alpha\beta \sum_{m=1}^{N_Y} B_{jm}^{(1)} \sum_{n=1}^{N_Z} C_{kn}^{(1)} W_{imn}$$

$$= \frac{2P_x(1-v)(1-2v)}{E} \left[\gamma^2 \sum_{l=1}^{N_x} A_{il}^{(2)} V_{ljk} + \phi\beta^2 \sum_{m=1}^{N_y} B_{jm}^{(2)} V_{imk} \right] \quad (17)$$

$$\gamma \sum_{l=1}^{N_X} A_{il}^{(1)} \sum_{n=1}^{N_Z} C_{kn}^{(1)} U_{ljn} + \gamma \sum_{m=1}^{N_Y} B_{jm}^{(1)} \sum_{n=1}^{N_Z} C_{kn}^{(1)} V_{imn} + \gamma^2(1-2v) \sum_{l=1}^{N_X} A_{il}^{(2)} W_{ljk}$$

$$+\beta^2(1-2v) \sum_{m=1}^{N_Y} B_{jm}^{(2)} W_{imk} + 2(1-v) \sum_{n=1}^{N_Z} C_{kn}^{(2)} W_{ijn}$$

$$= \frac{2P_x(1-v)(1-2v)}{E} \left[\gamma^2 \sum_{l=1}^{N_X} A_{il}^{(2)} W_{ljk} + \phi\beta^2 \sum_{m=1}^{N_Y} B_{jm}^{(2)} W_{imk} \right] \quad (18)$$

Using similar procedures, the stress–displacement equations [eqn 10a] can be discretised into the following equations:

$$\sigma_X = \gamma(1-v) \sum_{l=1}^{N_X} A_{il}^{(1)} U_{ljk} + \gamma v \sum_{m=1}^{N_Y} B_{jm}^{(1)} V_{imk} + v \sum_{n=1}^{N_Z} C_{kn}^{(1)} W_{ijn} \quad (19)$$

$$\sigma_Y = \gamma v \sum_{l=1}^{N_X} A_{il}^{(1)} U_{ljk} + \gamma(1-v) \sum_{m=1}^{N_Y} B_{jm}^{(1)} V_{imk} + v \sum_{n=1}^{N_Z} C_{kn}^{(1)} W_{ijn} \quad (20)$$

$$\sigma_Z = \gamma v \sum_{l=1}^{N_X} A_{il}^{(1)} U_{ljk} + \gamma v \sum_{m=1}^{N_Y} B_{jm}^{(1)} V_{imk} + (1-v) \sum_{n=1}^{N_Z} C_{kn}^{(1)} W_{ijn} \quad (21)$$

$$\alpha\tau_{XY} = \alpha^2 \sum_{m=1}^{N_Y} B_{jm}^{(1)} U_{imk} + \sum_{l=1}^{N_X} A_{il}^{(1)} V_{ljk} \quad (22)$$

$$\gamma\tau_{XZ} = \gamma \sum_{l=1}^{N_X} A_{il}^{(1)} W_{ljk} + \sum_{n=1}^{N_Z} C_{kn}^{(1)} U_{ijn} \quad (23)$$

$$\beta\tau_{YZ} = \sum_{n=1}^{N_Z} C_{kn}^{(1)} V_{ijn} + \alpha\beta \sum_{m=1}^{N_Y} B_{jm}^{(1)} W_{imk} \tag{24}$$

4.2. *Normalisation and discretisation of the boundary conditions*

The discretised edge and surface boundary conditions can be obtained by first substituting eqn (15) into eqns (11–14) then apply the DQ procedure. The discretised forms of the edge boundary conditions at $X =$ constant and the free surface boundary conditions at $Z = 0$ are given as follows:

- Clamped edge boundary condition (C)

$$U_{ijk} = 0; \quad V_{ijk} = 0; \quad W_{ijk} = 0 \tag{25a–c}$$

- Simply supported edge boundary condition (S)

$$\gamma v \sum_{l=1}^{N_X} A_{il}^{(1)} U_{ljk} + \gamma v \sum_{m=1}^{N_Y} B_{jm}^{(1)} V_{imk} + v \sum_{n=1}^{N_Z} C_{kn}^{(1)} W_{ijn} = 0; \tag{26a}$$

$$V_{ijk} = 0; \quad W_{ijk} = 0 \tag{26b–c}$$

- Free edge boundary condition (F)

$$\gamma(1-v) \sum_{l=1}^{N_X} A_{il}^{(1)} U_{ljk} + \gamma v \sum_{m=1}^{N_Y} B_{jm}^{(1)} V_{imk} + v \sum_{n=1}^{N_Z} C_{kn}^{(1)} W_{ijn} = 0; \tag{27a}$$

$$\alpha^2 \sum_{m=1}^{N_y} B_{jm}^{(1)} U_{imk} + \sum_{l=1}^{N_x} A_{il}^{(1)} V_{ljk} = 0; \tag{27b}$$

$$\gamma \sum_{l=1}^{N_X} A_{il}^{(1)} W_{ljk} + \sum_{n=1}^{N_Z} C_{kn}^{(1)} U_{ijn} = 0 \tag{27c}$$

- Free surface boundary condition

$$\gamma v \sum_{l=1}^{N_X} A_{il}^{(1)} U_{ljk} + \gamma v \sum_{m=1}^{N_Y} B_{jm}^{(1)} V_{imk} + (1-v) \sum_{n=1}^{N_Z} C_{kn}^{(1)} W_{ijn} = 0; \tag{28a}$$

$$\gamma \sum_{l=1}^{N_X} A_{il}^{(1)} W_{ljk} + \sum_{n=1}^{N_Z} C_{kn}^{(1)} U_{ijn} = 0; \tag{28b}$$

$$\sum_{n=1}^{N_Z} C_{kn}^{(1)} V_{ijn} + \alpha\beta \sum_{m=1}^{N_Y} B_{jm}^{(1)} W_{imk} = 0 \tag{28c}$$

4.3. *Solution procedures*

From the above procedures, one can derive the general form of eigenvalue equation as follows:

$$\mathbf{DU} = k\mathbf{EU} \tag{29}$$

where **D** and **E** are matrices derived from the governing eqns (23)–(25); and $\mathbf{U} = [U_{ijk} \quad V_{ijk} \quad W_{ijk}]^T$ is the displacement vector. In the above eigenvalue equation, k is the non-dimensional buckling factor used. It is defined as $k = P_x b^2 c/\pi^2 D$ where

$$D = \frac{Ec^3}{12(1-v^2)} \tag{30}$$

The determinant of the matrix to be solved for a solution domain with a grid size of $N_x \times N_y \times N_z$ is $(3 \times N_x \times N_y \times N_z)$. In forming the system of equations, the points on the six faces of the plate are described by the boundary conditions whereas the points inside the plate are described by the governing equations. For example, if $N_x = N_y = N_z = N$ is assumed, the solution domain of N^3 points has $(4N^2-6N+4)$ points being described by the boundary conditions. In other words, there are $(N-2)^3$ points in the solution domain that are described by the three governing equations.

5. Results and discussion

When the solution domain is discretised, one needs to determine the mesh pattern to be used. Two of the most commonly used mesh pattern are (i) the uniform mesh pattern, and (ii) the cosine mesh pattern. The uniform mesh pattern divides the solution domain into points equidistant to one another. The cosine mesh pattern, however, divides the solution domain into points following

Table 1
Convergence characteristic of the buckling factors, $k = P_x b^2 c/\pi^2 D$, of a uniaxially loaded simply supported square plate generated by the DQ method using the uniform mesh pattern and the cosine mesh pattern

Grid size	$c/b = 0.05$	$c/b = 0.1$	$c/b = 0.2$
	Uniform mesh pattern		
$5 \times 5 \times 5$	3.6800	3.5108	2.9803
$6 \times 6 \times 6$	3.7021	3.6056	3.1307
$7 \times 7 \times 7$	3.9467	3.7549	3.1627
$8 \times 8 \times 8$	3.9443	3.7475	3.1549
$9 \times 9 \times 9$	3.9310	3.7409	3.1531
$10 \times 10 \times 10$	3.9311	3.7411	3.1533
$11 \times 11 \times 11$	3.9314	3.7408	3.1527
	Cosine mesh pattern		
$5 \times 5 \times 5$	3.8636	3.6783	3.1036
$6 \times 6 \times 6$	3.8797	3.7052	3.1412
$7 \times 7 \times 7$	3.9329	3.7425	3.1542
$8 \times 8 \times 8$	3.9326	3.7419	3.1535
$9 \times 9 \times 9$	3.9314	3.7412	3.1533
$10 \times 10 \times 10$	3.9314	3.7412	3.1533
$11 \times 11 \times 11$	3.9314	3.7412	3.1533

the cosine function. Below is the formula showing the division of the axes into a cosine mesh pattern:

$$\Theta(i) = \frac{1}{2}\left(1 - \frac{\cos(i-1)\times\pi}{N-1}\right) \tag{31}$$

where $\Theta(i)$ can be the $x(i)$, $y(i)$ or $z(i)$ co-ordinate of the ith points considered.

Table 1 presents the buckling factor, $k = P_x b^2/\pi^2 D$, of a uniaxially loaded simply supported square plate computed using the uniform mesh pattern and the cosine mesh pattern. The thickness to width ratio, c/b, of the plate investigated here are 0.05, 0.1 and 0.2. It is observed that the DQ solution computed using the cosine mesh pattern converge up to at least the fifth significant figure for plate with all thickness to width ratios considered when the grid size is $9\times9\times9$. On the contrary, the DQ solution generated by the uniform mesh pattern only converge up to the fourth significant figure for plate with thickness to width ratio of 0.05 and 0.2, and the third significant figure for plate with thickness to width ratio of 0.1 when the grid size is $11\times11\times11$. From the above observations, one can conclude that the DQ method is mesh pattern dependent and the

Table 2
Convergence studies of buckling factors, $k = P_x b^2 c/\pi^2 D$, for a fully simply supported rectangular plate

Aspect ratio a/b	Grid number $X\times Y\times Z$	Uniaxial loading thickness ratio, c/b			Biaxial loading thickness ratio, c/b		
		0.05	0.10	0.15	0.05	0.10	0.15
0.5	$5\times5\times5$	5.8669	5.2368	4.4685	4.6933	4.1886	3.5736
	$6\times6\times6$	5.9078	5.3051	4.5403	4.7265	4.2443	3.6324
	$7\times7\times7$	5.9928	5.3435	4.5547	4.7943	4.2748	3.6438
	$8\times8\times8$	5.9915	5.3418	4.5533	4.7932	4.2734	3.6426
	$9\times9\times9$	5.9899	5.3412	4.5530	4.7919	4.2729	3.6424
	$10\times10\times10$	5.9899	5.3412	4.5530	4.7919	4.2729	3.6424
	$11\times11\times11$	5.9899	5.3412	4.5530	4.7919	4.2729	3.6298
1.0	$5\times5\times5$	3.8636	3.6783	3.4111	1.9318	1.8389	1.3642
	$6\times6\times6$	3.8797	3.7052	3.4457	1.9398	1.8524	1.3781
	$7\times7\times7$	3.9329	3.7425	3.4687	1.9664	1.8713	1.3875
	$8\times8\times8$	3.9326	3.7419	3.4680	1.9663	1.8710	1.3872
	$9\times9\times9$	3.9314	3.7412	3.4676	1.9657	1.8706	1.3871
	$10\times10\times10$	3.9314	3.7412	3.4676	1.9657	1.8706	1.3871
	$11\times11\times11$	3.9314	3.7412	3.4676	1.9657	1.8706	1.3871
1.5	$5\times5\times5$	4.5491	4.3882	4.1475	1.3997	1.3501	1.2759
	$6\times6\times6$	4.1892	3.9263	3.5613	1.4049	1.3594	1.2886
	$7\times7\times7$	4.1965	3.9309	3.5626	1.4271	1.3761	1.2999
	$8\times8\times8$	4.2445	3.9671	3.5873	1.4270	1.3758	1.2996
	$9\times9\times9$	4.2436	3.9653	3.5851	1.4264	1.3755	1.2994
	$10\times10\times10$	4.2374	3.9612	3.5826	1.4264	1.3755	1.2994
	$11\times11\times11$	4.2375	3.9613	3.5827	1.4265	1.3755	1.2994

Table 3
Convergence studies of buckling factors, $k = P_x b^2 c/\pi^2 D$, for a fully clamped rectangular plate subject to biaxial loading ($1.5P_x = P_y$)

Aspect ratio a/b	Grid number $X \times Y \times Z$	Thickness ratio c/b		
		0.05	0.10	0.15
0.5	$5\times5\times5$	15.828	10.907	7.3330
	$6\times6\times6$	14.194	9.6919	6.5982
	$7\times7\times7$	12.400	9.0198	6.2066
	$8\times8\times8$	11.921	8.5177	5.9344
	$9\times9\times9$	11.899	8.5010	5.9162
	$10\times10\times10$	11.869	8.4839	5.9061
	$11\times11\times11$	11.862	8.4809	5.9035
1.0	$5\times5\times5$	5.0368	4.3260	3.5322
	$6\times6\times6$	4.8508	4.0417	3.2560
	$7\times7\times7$	4.0646	3.5631	2.9870
	$8\times8\times8$	4.0586	3.5581	2.9839
	$9\times9\times9$	4.0539	3.5558	2.9829
	$10\times10\times10$	4.0490	3.5511	2.9799
	$11\times11\times11$	4.0358	3.5494	2.9794
1.5	$5\times5\times5$	3.7524	3.2988	2.7663
	$6\times6\times6$	3.6079	3.0760	2.5423
	$7\times7\times7$	2.9677	2.6712	2.3071
	$8\times8\times8$	2.9643	2.6685	2.3053
	$9\times9\times9$	2.9612	2.6666	2.3043
	$10\times10\times10$	2.9579	2.6630	2.3017
	$11\times11\times11$	2.9537	2.6614	2.3011

cosine mesh pattern provides better convergence characteristics when compared to the uniform mesh pattern. It is decided that throughout this paper, the cosine mesh pattern shall be used for the computation of results.

Several plate problems are considered herein. Before we can start presenting some new results, further studies on the convergence characteristics and validity of the method need to be done. Convergence studies have been carried out for the SSSS plate under uniaxial and biaxial loading. For the biaxial loading, the value of ϕ is set to unity. These results are tabulated in Table 2. The convergence study of the CCCC plate under biaxial loading with $\phi = 1.5$ is also studied. The results are tabulated in Table 3.

In Table 2, one can observe that the solutions for both the uniaxially and biaxially loaded SSSS plate with the aspect ratios $a/b = 0.5$ and 1.0 converge to five significance figures when the solution grid size reach $9\times9\times9$. This also applies to the SSSS plate with aspect ratio of 1.5 under the biaxial loading. For a uniaxially loaded SSSS plate of aspect ratio 1.5, the buckling load converges to four significant figures when the solution grid size is $10\times10\times10$. Hence, one can safely conclude that both the uniaxially and biaxially loaded SSSS plates can converge to at least the fourth

significant figure at the grid size of $10 \times 10 \times 10$. From Table 3, one can see that the buckling load factors for the CCCC plate under the biaxial loading converge to three significance figures for aspect ratios ranging from 0.5–1.5, and the thickness to width ratios ranging from 0.05–0.15. It is thus concluded that for the biaxially loaded CCCC plate, the results converge to at least 3 significant figures at the grid size of $10 \times 10 \times 10$.

Some comparison studies are also carried out to validate the accuracy of the method. The DQ solutions generated are compared to results produced by other researchers, namely Xiang (1993); Hinton (1988); Roufaeil and Dawe (1982); Srinivas and Rao; (1969, 1970); and Timoshenko and Gere (1961). In this study, the percentage error is determined based on the following expressions:

$$\% \text{ deviation} = \left| \left(\frac{\text{present solution} - \text{published solution}}{\text{published solution}} \right) \times 100 \right| \tag{32}$$

Table 4 shows the comparison studies of a uniaxially loaded SSSS plate. The present solution of plate with thickness to width ratio of 0.01, 0.05, 0.1, and 0.2 were compared with solutions from the Classical plate theory, the Mindlin plate theory, and the three-dimensional elasticity solution. They were found to be in good agreement. When the present solution is compared with the analytical three-dimensional solution (Srinivas and Rao, 1969), the greatest deviation is 0.5%. It was hence verified that the present DQ solution is correct and accurate.

Table 5 shows the comparison studies with the closed form solution (Hinton, 1978) and the *p*-Ritz solution (Xiang, 1993) of a biaxially loaded SSSS plate with $P_x = P_y$. When the DQ solutions are compared to these two solutions, one can deduce that as the aspect ratio changes from 1.0–2.0, the greatest percentage deviation is 2.84% whereas the lowest percentage deviation is 0.75%. Table 6 gives the comparison of a uniaxially loaded CCCC plate. It shows the solutions for plates with aspect ratios of 0.5, 1.0, 1.5 and 2.0, and thickness to width ratios of 0.05, 0.1, 0.15 and 0.2. These results are compared with the *p*-Ritz solutions of Reissner/Mindlin plates (Xiang, 1993). Of the above comparisons, plates with aspect ratio $a/b = 2$, has the least deviation. Of the solutions compared, the worst case comes from plates with aspect ratio $a/b = 0.5$ which shows a percentage deviation of about 4.6%. Table 7 compares the DQ solution of a uniaxially loaded SFSF plate with the results generated by the *p*-Ritz method based on the Reissner/Mindlin plate theory (Xiang,

Table 4
Comparison study of buckling factors, $k = P_x b^2 c/\pi^2 D$, for a full simply supported square plate under uniaxial loading

Researchers	C/b			
	0.01	0.05	0.1	0.2
Present solution	4.020	3.931	3.741	3.153
Xiang (1993)	—	3.944	3.786	3.264
Hinton (1988)	—	3.944	3.786	3.264
Roufaeil and Dawe (1982)	—	3.929	3.731	—
Srinivas and Rao (1969)	—	3.911	3.741	3.150
Timoshenko and Gere (1961)	4.000	—	—	—

Table 5
Comparison study of buckling factors, $k = P_x b^2 c/\pi^2 D$, for a fully simply supported rectangular plate under biaxial loading ($c/b = 0.1$)

Researchers	a/b				
	1.00	1.25	1.50	1.75	2.00
Present solution	1.871	1.552	1.376	1.268	1.198
Xiang (1993)	1.893	1.568	1.338	1.279	1.207
Hinton (1988)	1.893	1.568	1.338	1.279	1.207

Table 6
Comparison study of buckling factors, $k = P_x b^2 c/\pi^2 D$, for a fully clamped rectangular plate subjected uniaxial loading

a/b	Method of solution	c/b			
		0.05	0.1	0.15	0.2
0.5	Present	16.954	12.476	8.8623	6.3903
	Xiang (1993)	17.222	13.026	9.2881	6.6166
1.0	Present	9.5514	8.1391	6.5449	5.1166
	Xiang (1993)	9.5588	8.2917	6.7595	5.3156
1.5	Present	7.9931	6.8891	5.6601	4.5691
	Xiang (1993)	7.9431	6.9608	5.8012	4.7156
2.0	Present	7.5923	6.5668	5.4254	4.4127
	Xiang (1993)	7.4870	6.5736	5.5013	4.5026
2.5	Present	7.5126	6.5866	5.5132	4.5269
	Xiang (1993)	7.2304	6.3908	5.3629	4.4033

Table 7
Comparison study of buckling factors, $k = P_x b^2 c/\pi^2 D$, for a full SFSF rectangular plate under uniaxial loading

c/b	Method of solution	a/b				
		1.00	1.25	1.50	1.75	2.00
0.10	Present	0.9162	0.5887	0.4090	0.3002	0.2296
	Xiang (1993)	0.9223	0.5913	0.4103	0.3009	0.2036
0.15	Present	0.8785	0.5725	0.4009	0.2958	0.2270
	Xiang (1993)	0.8908	0.5779	0.4036	0.2972	0.2278

1993). For the plate with thickness to width ratio of 0.1, and aspect ratios ranging from 1.0–2.0, the percentage deviation of the present results from those of the *p*-Ritz solutions are less than 0.7%. For the plate with thickness to width ratio of 0.15, the percentage deviation is less than 1.4%.

The comparison shown in Tables 5–7 reveals some percentage deviations which could be due to two reasons. The first reason is, the *p*-Ritz method used by Xiang (1993) is a numerical approach. Therefore, the results presented by Xiang (1993) in Tables 5–7 would have some numerical error. Similarly the results generated by the DQ method also have induced some numerical error. The numerical error contributed by both methods thus plays a part in the percentage deviation. The second reason which contributes to the percentage deviations is from the fact that the theory used for the solutions by Xiang (1993) and Hinton (1978) were based on the Mindlin plate theory, whereas the DQ results generated in the present study is based on the three-dimensional elasticity theory. In this case, one would expect some discrepancies in the comparison studies as the theories used are different.

Figure 3 presents the relationship between the buckling load factor, k, and the aspect ratio of

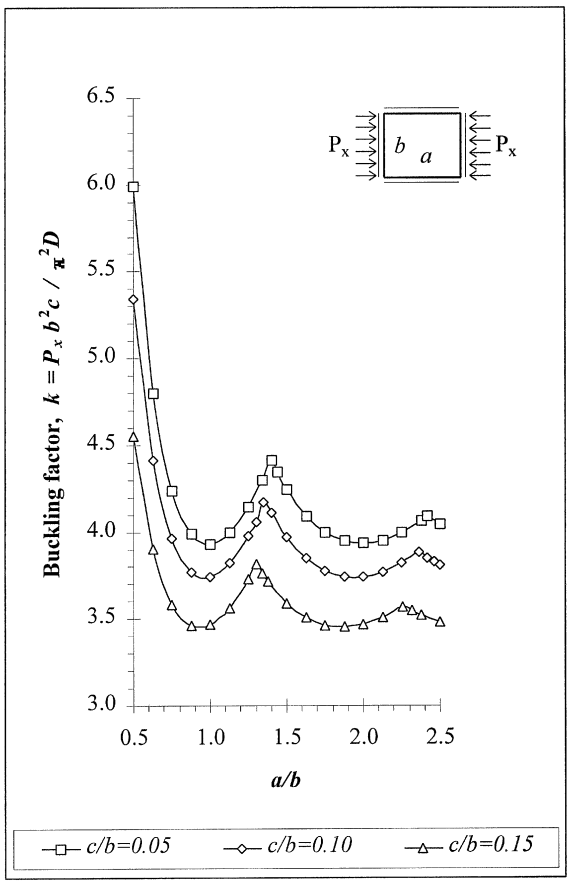

Fig. 3. Buckling factor, $k = P_x b^2 c/\pi^2 D$, vs aspect ratio, a/b, for SSSS plates subject to uniaxial loadings.

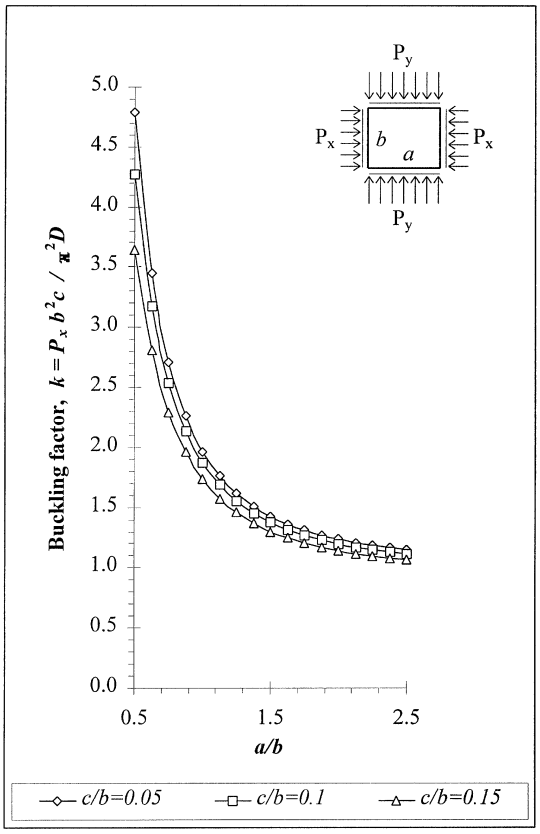

Fig. 4. Buckling factor, $k = P_x b^2 c/\pi^2 D$, vs aspect ratio, a/b, for SSSS plates subject to biaxial loadings, $P_x = P_y$.

an SSSS plate subject to uniaxial loading. Figures 4 and 5 present the relationship between the buckling load factor and the aspect ratio of SSSS and CCCC plates subject to biaxial loading with $P_x = P_y$. Results of different thickness to width ratios are also presented. From Figs 4 and 5, one can observe that for plates subject to biaxial loading, the buckling factor decreases as the plate aspect ratio decreases. Figure 6 shows the relationship between the buckling load factor, k, and the aspect ratio of the CCCC plate subject to biaxial loading. In this figure, various ratios of the buckling load in the x and y directions are considered. From the figure, one can conclude that as the ratio P_x: P_y is reduced, the buckling load factor decreases for $\phi \geqslant 1$. This is because as the ratio P_x: P_y is reduced, the effect of P_y becomes more pronounced over P_x. When $\phi < 1$, one can observe that there is a mode shift as the aspect ratio increases. Hence, the buckling load factor k being expressed in terms of P_x is reduced. Figure 7 shows the relationship between the buckling load factor k, and the plate aspect ratio of the SFSF plate subject to uniaxial loading. It is observed that as the aspect ratio increases, the buckling load factor for different thickness to width ratio converges. This effect is more pronounced when the plate aspect ratio is greater than 1.5.

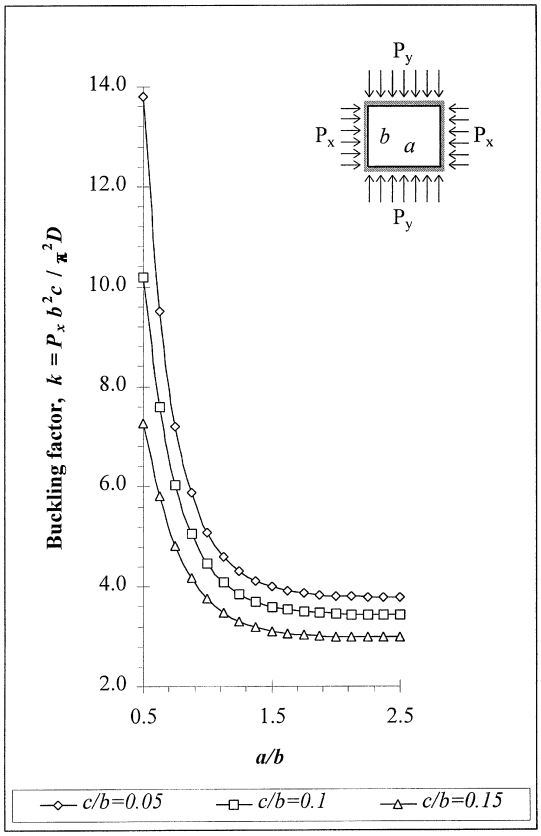

Fig. 5. Buckling factor, $k = P_x b^2 c/\pi^2 D$, vs aspect ratio, a/b, for CCCC plates subject to biaxial loadings, $P_x = P_y$.

6. Concluding remarks

This paper presented the first known application of the DQ method to the elastic plate buckling problem using the three-dimensional elasticity theory. The convergence characteristics of the method for various problems were studied and two conclusions were drawn. The first is the convergence characteristic of the DQ method is mesh dependent. In this study, the cosine mesh pattern yields a more stable convergence characteristic than the uniform mesh pattern. The second is a relatively coarse mesh used in the solution domain of the DQ method was sufficient to produce convergence and accurate results. In addition, examples of uniaxially and biaxially loaded plates constrained by simply supported, clamped and free boundary conditions were studied by varying the ratio of the destabilising effect in the x-direction to that of the y-direction, their thickness to width ratio, and their aspect ratio.

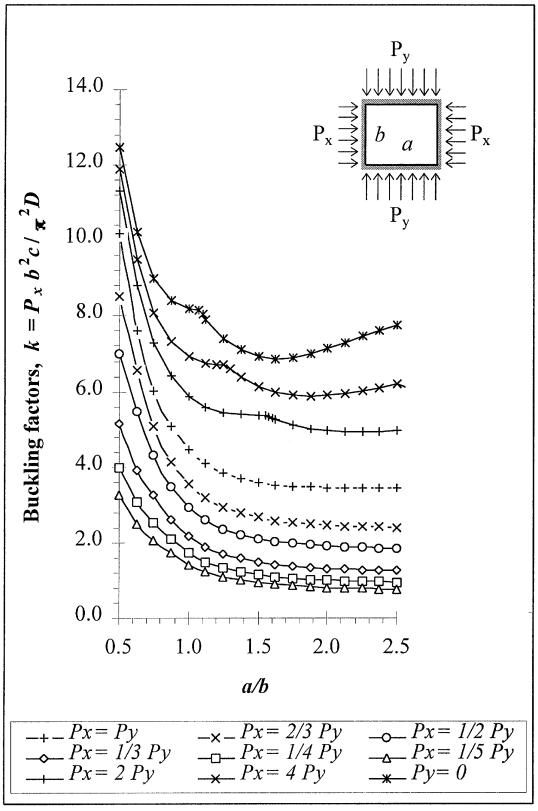

Fig. 6. Buckling factor, $k = P_x b^2 c/\pi^2 D$, vs aspect ratio, a/b, for CCCC plates with thickness ratio, $c/b = 0.1$, subject to biaxial loadings.

References

Bellman, R. (1973) *Methods of Nonlinear Analysis*. Academic Press, New York.

Benson, P. R. and Hinton, E. (1976) A thick finite strip solution for static, free vibration and stability problems. *International Journal of Numerical Methods in Engineering* **10,** 665–678.

Bert, C. W. and Chang, S. (1972) Shear-flexible orthotropic plates loaded in plane. *Journal of Engineering Mechanics* **98,** 1499–1509.

Bert, C. W., Jang, S. K. and Striz, A. G. (1988) Two new approximate methods for analyzing free vibration of structural components. *American Institute of Aeronautics and Astronautics Journal* **26,** 612–618.

Bert, C. W., Jang, S. K. and Striz, A. G. (1989) Nonlinear bending analysis of orthotropic rectangular plates by the method of differential quadrature. *Computational Mechanics* **5,** 217–226.

Brunelle, E. J. (1971) Buckling of transversely isotropic Mindlin plates. *American Institute of Aeronautics and Astronautics Journal* **9,** 1018–1022.

Cheung, Y. K., Chan, A. H. C. and Tham, L. G. (1986) A study of the linear elastic stability of Mindlin plates. *International Journal of Numerical Methods in Engineering* **22,** 117–132.

Civan, F. and Sliepcevich, C. M. (1983) Application of differential quadrature to transport processes. *Journal of Mathematical Analysis and Applications* **93,** 206–221.

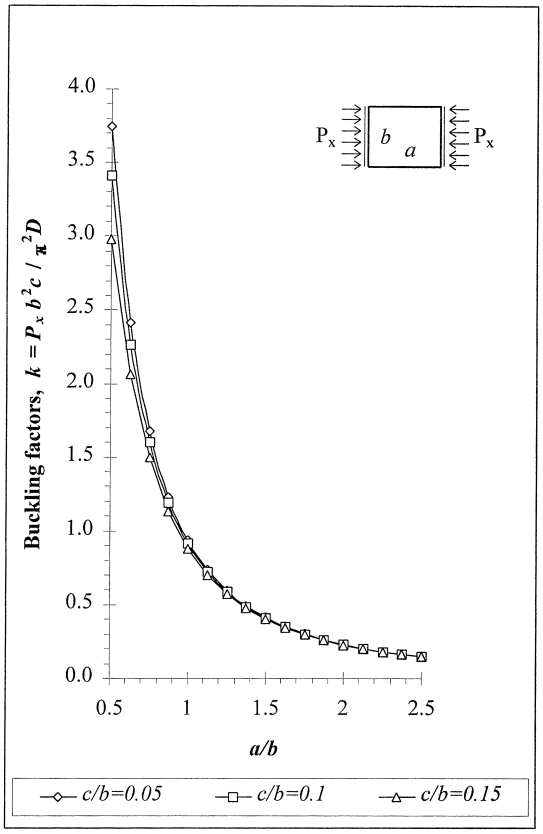

Fig. 7. Buckling factor, $k = P_x b^2 c/\pi^2 D$, vs aspect ratio, a/b, for SFSF plates subject to uniaxial loadings.

Civan, F. and Sliepcevich, C. M. (1984) Differential quadrature for multi-dimensional problems. *Journal of Mathematical Analysis and Applications* **101,** 423–443.

Doong, J. L. (1987) Vibration and stability of an initially stressed thick plate according to a high-order deformation theory. *Journal of Sound and Vibration* **113,** 425–440.

Du, H., Liew, K. M. and Lim, M. K. (1996) Generalized differential quadrature method for buckling analysis. *Journal of Engineering Mechanics* **122**(2), 95–100.

Han, J.-B. and Liew, K. M. (1997) An eight-node curvilinear differential quadrature formulation for Reissner/Mindlin plates. *Computer Methods in Applied Mechanics and Engineering* **141,** 265–280.

Hinton, E. (1978) Buckling of initially stressed Mindlin plates using a finite strip method. *Computers and Structures* **8,** 99–105.

Hinton, E. (1988) *Numerical Methods and Software for Dynamic Analysis of Plates and Shells*. Pineridge Press, Swansea, U.K.

Hutchinson, J. R. and Zillimer, S. D. (1983) Vibration of a free rectangular parallelepiped. *Journal of Applied Mechanics* **50,** 123–130.

Iyengar, K. T., Chandrashekhara, K. and Sebastian, V. K. (1974) On the analysis of thick rectangular plates. *Ingenieur Archiv* **43,** 317–339.

Leissa, A. W. and Zhang, Z. D. (1983) On the three-dimensional vibrations of the cantilevered rectangular parallelepiped. *Journal of Acoustical Society of America* **73,** 2013–2021.

Liew, K. M., Hung, K. C. and Lim, M. K. (1993) A continuum three-dimensional vibration analysis of thick rectangular plates. *International Journal of Solids and Structures* **30,** 3357–3379.

Liew, K. M., Hung, K. C. and Lim, M. K. (1994) Three-dimensional vibratio of rectangular plates: variance of simple support conditions and influence of in-plane inertia. *International Journal of Solids and Structures* **31,** 3233–3247.

Liew, K. M., Hung, K. C. and Lim, M. K. (1995) Free vibration studies on stress-free three-dimensional elastic solids. *Journal of Applied Mechanics* **62,** 159–165.

Liew, K. M. and Han, J. B. (1997) A four node differential quadrature method for straight-sided quadrilateral Reissner/Mindlin plates. *Communications in Numerical Methods in Engineering* **13**(2), 73–81.

Liu, F., Liew, K. M. and Han, J. B. (1997) Development of differential quadrature element method for vibration analysis of Mindlin plates. *The 7th International Conference on Computing in Civil and Building Engineering*, 19–21 August 1997. Seoul, Korea.

Pagano, N. J. (1970) Exact solutions for rectangular bidirectional composites and sandwich plates. *Journal of Composite Materials* **5,** 20–34.

Quan, J. R. and Chang, C. T. (1989a) New insights in solving distributed system of equations by the quadrature method—I. Analysis. *Computers in Chemical Engineering* **13,** 779–788.

Quan, J. R. and Chang, C. T. (1989b) New insights in solving distributed system of equations by the quadrature method—II. Numerical experiments. *Computers in Chemical Engineering* **13,** 1017–1024.

Rao, R. V., Venkataramana, J. and Raju, K. K. (1975) Stability of moderately thick rectangular plates using a high precision triangular element. *Computers and Structures* **5,** 257–259.

Roufaeil, O. L. and Dawe, D. J. (1982) Rayleigh–Ritz vibration analysis of rectangular Mindlin plates subjected to membrane stresses. *Journal of Sound and Vibration* **85,** 263–275.

Shu, C. and Richards, B. E. (1992) Application of generalized differential quadrature to solve two-dimensional incompressible Navier–Stokes equations. *International Journal for Numerical Methods in Fluids* **15,** 791–798.

Srinivas, S. and Rao, A. K. (1969) Buckling of thick rectangular plates. *American Institute of Aeronautics and Astronautics Journal* **7,** 1645–1646.

Srinivas, S. and Rao, A. K. (1970) Bending, vibration and buckling of simply supported thick orthotropic rectangular plates and laminates. *International Journal of Solids and Structures* **6,** 1463–1481.

Timoshenko, S. P. and Gere, J. M. (1961) *Theory of Elastic Stability*. McGraw-Hill, New York, N.Y.

Wang, C. M., Liew, K. M., Xiang, Y. and Kitipornchai, S. (1993) Buckling of rectangular Mindlin plates with internal line supports. *International Journal of Solids and Structures* **30,** 1–17.

Wittrick, W. H. (1987) Analytical, three-dimensional elasticity solutions to some plate problems, and some observations on Mindlin's plate theory. *International Journal of Solids and Structures* **23**(4), 441–464.

Xiang, Y. (1993) Numerical developments in solving the buckling and vibration of Mindlin plates. Ph.D. thesis, The University of Queensland, Australia.

Young, P. G. and Dickinson, S. M. (1995) Free vibration of a class of homogeneous isotropic solids. *Journal of Applied Mechanics* **62,** 706–708.